JOURNAL OF MATERIALS SCIENCE 23 (1988) 72–82

Shear strength of highly drawn linear polyethylene sheets

N. H. LADIZESKY*, I. M. WARD
Department of Physics, University of Leeds, Leeds LS2 9JT, UK

The shear strength of highly drawn linear polyethylene (HDLPE) sheets has been measured using sample shapes suggested by the lap joint technique. Several variables were investigated, including different parent polymers, irradiation dose, draw ratio, drawing methods and geometrical parameters. The lap joint theory has been successfully applied to several qualitative aspects of these experiments.

1. Introduction

During the last few years our laboratories have given considerable attention to the production, study and application of highly drawn linear polyethylene (HDLPE) sheets and fibres. With special production methods these materials may be drawn to levels well above their "natural" draw ratio of about 8 and these techniques are well documented in the literature [1].

HDLPE materials show interesting possibilities in a number of applications. These include structural materials of interest to the civil engineer, the aerospace and automotive industry, dental and orthopaedic components, barrier materials to control diffusion of gases, bullet-proof structures, etc. It is therefore important to characterize HDLPE as thoroughly as possible, and special attention has been given to the mechanical properties and their relationship with morphology.

HDLPE may be produced in a wide variety of forms, including multifilament and monofilament fibres [2, 3], and in solid sections such as sheets, rods and tubes [4, 5]. The properties of the drawn material are broadly independent of the production methods, as long as some essential parameters are kept constant. These parameters may be related to the parent material, e.g. molecular weight, or to the final material. In the latter case the most important parameter is the draw ratio, that is, the final length divided by the original length of a given portion of the material. Attention should also be given to the stress field applied to the material during drawing. For example, during the production of highly drawn multifilament and monofilament fibres the stresses responsible for the deformation are solely uniaxial. For the drawing of sheets, on the other hand, the stress system may be more accurately regarded as biaxial. These differences will affect the morphology of the final product and, to a smaller extent, its mechanical properties.

The different methods of fabrication and the associated variety of shapes of the final product allow the characterization of HDLPE material over a wide range of modes of deformation. Although the different products may not be fully comparable in some areas such as morphology, the mechanical properties obtained from them will form a qualitative self-consistent description of the behaviour of HDLPE, and this will be particularly useful to study the dependence of those properties on variables such as draw ratio, molecular weight, time dependence, etc.

In the past we have studied the development of adhesion of very highly drawn monofilament and multifilament fibres to polymeric resins [6]. It was found that plasma treatment of the fibres using oxygen gas as the plasma carrier produced higher adhesion and, in this case, the system failed through a peeling-off mechanism of the fibres, mostly by shear.

It is therefore of considerable technological importance to study the shear failure behaviour of HDLPE. Because there are obvious difficulties to carry out this work on fibres it was decided to study material of similar structure and properties in sheet form.

It is the purpose of this study to measure the shear strength of HDLPE sheets. Attention has been given to the effect of strain rate and initial draw ratio as well as to the possibility of increasing the shear strength of HDLPE material by the introduction of cross-links produced by irradiation, either before or after drawing.

2. Experimental details

2.1. Materials and production of the sheets

Two linear polyethylenes were used for this work: Hizex 7000F, $\bar{M}_w = 318\,000$, $\bar{M}_n = 15\,100$, made by Mitsui Petrochemical Industries Ltd, Japan, and BP006/60, $\bar{M}_w = 135\,000$, $\bar{M}_n = 25\,500$, made by BP Chemicals Ltd, UK.

Two methods of drawing were used.

(a) Tensile drawing: polymer granules were melted, platen pressed and quenched in water. Samples 8 cm long × 10 cm wide were cut into a dumb-bell shape with a parallel gauge 8 cm wide × 2 cm long. These samples were stamped with a square grid and stretched in an Instron machine at 10 cm min^{-1} and 75° C for

Present address: University of Hong Kong, Dental Materials Science Unit, The Prince Philip Dental Hospital, 34 Hospital Road, Hong Kong.

0022–2461/88 $03.00 + .12

BP006/60 and 115° C for Hizex 7000F. (The higher temperature for the latter material was required in order to avoid stress-whitening [7]. This was probably due to the high molecular weight of the polymer.) The draw ratio was then determined from the grid dimensions.

(b) Die drawing: for drawn sheets up to 0.5 mm thickness the polymer granules were platen pressed and quenched as described in (a). The isotropic sheets were die-drawn between 5 cm diameter stationary heated rollers used as a slot-die with a gap approximately 0.6 mm. For drawn sheets with a final thickness greater than 0.5 mm the polymer was screw-extruded into a mould, slow cooled and then machined into rectangular section billets, typically 62 mm broad and 20 mm thick. The billets were die drawn in a slot-die of constant breadth of aperture 63 mm but uniformly reducing height (semi-angle of 15°). The exit aperture of the die was 63 mm × 3.5 mm.

In both cases the die and billet were heated to temperatures between 90 and 105° C and the sheets were pulled through the gap at speeds varying between 5 and 20 cm min^{-1} according to the desired draw ratio; the faster rate of drawing producing a greater draw ratio.

The draw ratio of the die drawn sheets is given by the cross-section of the undrawn sheet divided by the cross-section of the drawn sheet, assuming no change of volume during the drawing process.

For this study we consider samples with thickness between 0.6 and 3.20 mm.

2.2. Irradiation of the sheets

Some sheets were irradiated in vacuum ($\simeq 0.1$ torr) either before or after drawing, using a sealed glass tube with 3 mm wall thickness. Two dose rates were used, namely 0.55 Mrad min^{-1} (high dose rate) and 0.0022 Mrad min^{-1} (low dose rate).

For the high dose rate we used a Van der Graaf electron beam accelerator, Type KS3000 made by High Voltage Engineering (Europe) N.V. The accelerating voltage was 2.9 MV and the irradiation homogeneity over the sample was $\pm 8\%$. To ensure homogeneous irradiation throughout the thickness the samples were turned over halfway through the total irradiation time.

The irradiation method described above is suitable for irradiation doses up to 10 Mrad. No attempt was made to control the temperature of irradiation, but the glass tubes and the samples inside could always be comfortably touched by hand immediately after irradiation. On the other hand, for doses between 15 and 30 Mrad significant heating occurred, although never above 120° C because no evidence of shrinkage or melting was found. However, these high irradiation doses produced elongated bubbles within the bulk of the drawn sheets (isotropic sheets were opaque). The length of these bubbles lies perpendicular to the orientation direction, and they are probably produced by evolution of hydrogen during irradiation. (For high irradiation dose the diffusion rate of the gas cannot compensate the production rate).

Satisfactory sheets with high irradiation dose were obtained with a cobalt source giving low γ-irradiation dose rates. The samples were again enclosed in a sealed 3 mm thick wall tube under vacuum, and the dose was accurate within $\pm 10\%$. A dose of 40 Mrad was obtained with no indication of bubbles or heating. The irradiation was carried out at room temperature.

2.3. Measurement of shear strength

The sample shape was designed to ensure that simple shear occurs in a plane parallel to the initial draw direction, i.e. parallel to the principal orientation direction. Initially, it was considered that a double yoke sample, as shown in Fig. 1a, would be most appropriate because this would avoid bending in the plane of the sheet. It was soon found, however, that it was impracticable to use samples of this shape because it is not possible to ensure that the two shear failures initiate simultaneously. It was therefore decided to examine the behaviour of a single simple shear sample as shown in Fig. 1b, and subsequently a modified sample which was easier to machine, as shown in Fig. 1c. Preliminary experiments showed that both shapes (b) and (c) bend in their own plane under stress, and both produce values for shear strength which are identical within the experimentally observed scatter. For convenience therefore, all the final experiments were performed with shape (c).

The shear strength measurements were carried out using an Instron tensile testing machine, Type TT-B. The bottom end of the vertical sample was rigidly clamped to the Instron cross-head. Samples of thickness greater than 0.5 mm were also rigidly clamped to the load cell, with a rigid link to minimize the

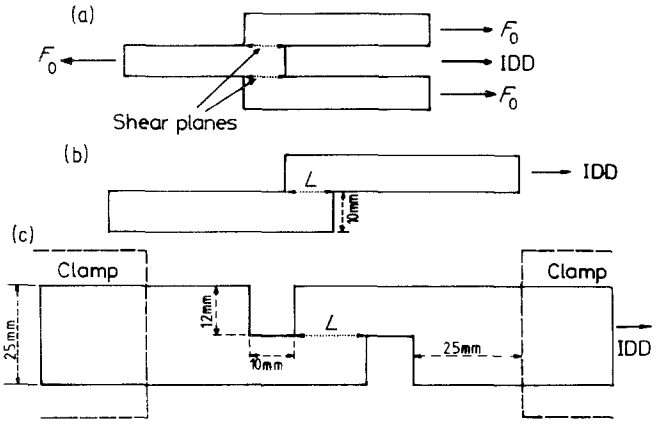

Figure 1 Different shapes of the shear samples. (a) Symmetrical, or double lap joint, (b) lap joint, (c) modified lap joint, as used in our experiments.

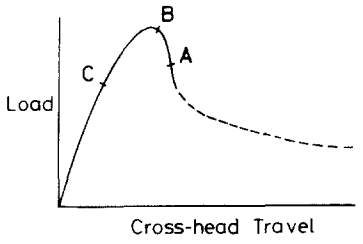

Figure 2 Typical load–deformation plot for the shear experiments.

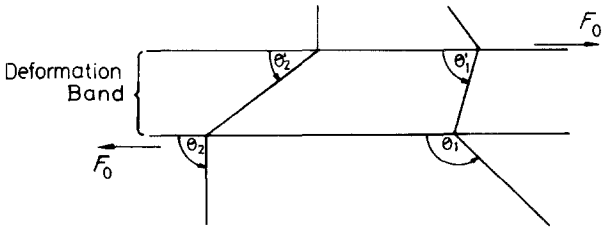

Figure 3 Calculation of shear strain γ. Definition of angles, indicating their positive sense.

bending of samples in their own plane. This procedure decreased the risk of splitting the samples, which was occasionally observed for the largest values of L (see Fig. 1 for nomenclature) when the top clamp and the load cell were joined by a universal link. Preliminary measurements using identical samples but different links showed that varying these clamping arrangements produced no detectable systematic changes in the values of shear strengths.

For samples with thickness 0.5 mm and less it was not possible to use a rigid link. To prevent samples bending away from the plane of the sheet during the test, the shear regions of the samples including the slots (see Fig. 1c) were sandwiched between two flat Perspex sheets of thickness 4 mm. The sandwich was held together by a rubber band. It was found that sliding the Perspex sheets over the samples generated a frictional load of about 0.5 N which was about twenty times smaller than the minimum load of 10 N applied to produce shear yielding in the samples.

The load–deformation curves obtained showed a distinctive yield point in all instances. A typical result is shown in Fig. 2. The shear strength was calculated as maximum load/Lw, where L is the length of the simple shear region and w is the thickness of the sheet.

Most of the shear strength measurements were performed at 22.0 $\pm$ 1.5° C. However, several identical samples were measured over the temperature range 18 to 26° C, and showed that the shear strength of the LPE sheets had a temperature dependence of 0.6 MPa ° C^{-1}. It was found that the scatter in the data could be reduced by correcting all the data to a single temperature. To make comparison easier with other laboratories, all our results are corrected to 20.0° C.

2.4. Measurement of strain

In all cases the shear deformation was contained within a very narrow band (L in Fig. 1) about 1 mm wide. This is called a "deformation band" or "band", by analogy with broadly similar observations made by Brown and Ward [8]. The simple shear strain γ, such that the only undistorted unrotated length is parallel to the deformation band, was measured by a method based on the previous work [8]. A fine shallow grid of parallel lines in two different directions was scratched on one surface of the undeformed samples, crossing the length where the band will be formed. Tests with thin samples scratched with different number of lines, and also unscratched, showed that the scratches had no effect on the shear strength, stress–strain curve, the strain, or any other feature of the deformation.

On formation of a deformation band, the changes of direction of two lines drawn on the sample are given by four quantities, m_1, m_2, m_1' and m_2', such that:

$$m_1 = \tan \theta_1 \qquad m_1' = \tan \theta_1'$$

$$m_2 = \tan \theta_2 \qquad m_2' = \tan \theta_2'$$

where θ_1 and θ_2 are the angles between the lines in the undeformed region and the band direction, and θ_1' and θ_2' are the corresponding angles in the deformed region, that is, within the deformation band. The diagram in Fig. 3 visualizes this situation. It can be shown [9]:

$$\gamma = \frac{m_2' m_1 - m_1' m_2}{(m_1 - m_2) m_1' m_2'}$$

By differentiating this equation with respect to each of the four variables θ_1, θ_2, θ_1', θ_2' it may be seen that γ is less sensitive to the errors affecting the measurement of the angles when $\theta_1 = 90°$ and $\theta_2 = 135°$ (positive sense as shown in Fig. 3). These two sets of directions were therefore chosen for all our samples.

As will be seen later, it was found that the shear strain γ within the band varies both along the band direction and across it. This variation was mapped out by scratching about ten approximately parallel lines for each set of directions, covering the whole length L of the band. Thus, to calculate the strain at a given point of the deformation band it was always possible to find two lines of different directions, passing sufficiently close to the chosen point.

The angles θ_1, θ_1', etc were measured with a polarizing microscope.

2.5. Measurement of the direction of the deformation band

From the geometry of the samples (Fig. 1) it is expected that the deformation band would be parallel to the initial draw direction (IDD). However, this was difficult to check visually because the band was not readily distinguishable from the material surrounding it. The direction of the band was therefore measured relative to the IDD, using the following method.

The IDD is parallel to the extinction direction outside the deformation band, as determined with a polarizing microscope, and this may also be revealed by the direction of surface flaws which are extended by the drawing process.

Contrary to most of the observations presented by Brown, Ward, Duckett and co-workers [8–12], the deformation bands in our experiments do not usually show a clear boundary. Fig. 4 shows the variation of the shear strain γ along a line (Y-direction) perpendicular to the IDD. The origin is an arbitrary point

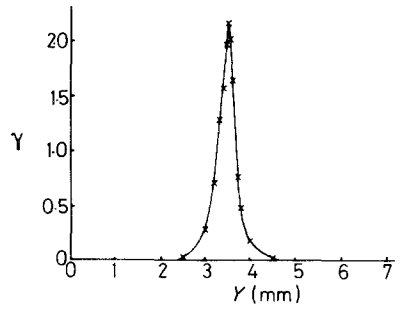

Figure 4 Variation of the shear strain γ across the deformation band. Y is perpendicular to the IDD, and in the plane of the sheet.

outside the band. It can be seen that the shear strain increases gradually, reaches a maximum and then decreases. To a good approximation the curve is symmetrical relative to its maximum. This type of curve was observed for every tested sample, and lead us to define the band direction as follows: consider the axes X and Y in the plane of the sheet, with X being parallel to the IDD and Y perpendicular to it. X is zero at one of the edges of the band, and increasing towards the other end. The origin of Y is arbitrary, but preferably outside the band. In this system we plot the coordinates of the maxima of the shear strain along the length of the band. The result of such a procedure may be seen in Fig. 5, where the line DB joining the points defines the direction of the band, relative to the IDD. Fig. 5 corresponds to a sample with a DB–IDD angle of 0.7°. Although values up to 3.4° were encountered, for most samples this angle was below 1.0°.

2.6. Other techniques

For some experiments the shear deformation was continued until the two sides of the samples came apart. The surfaces of the shear region were then examined in the scanning electron microscope (SEM). The instrument was a Cambridge Stereoscan 150 MkII. The samples were gold-coated with a Polaron 500 Vacuum Coating Unit, run at 1.2 kV and 10 A for 8 min, to obtain a gold layer about 20 μm thick with a negligible temperature increase. Particular attention was given to the choice of the SEM parameters, in order to avoid electron beam damage of the specimens.

3. Results and discussion

3.1. Shear strength measurements: general considerations

We have studied the effect of several variables on the shear strength of the sheets, namely the draw ratio, method of drawing, strain rate, material, and electron irradiation either before or after drawing. Furthermore, in an effort to ensure that the results obtained reflect material properties, we also studied the effect of geometrical variables such as the sample thickness and the length L of the deformation band.

The largest single group of samples was drawn between 10.0 : 1 and 11.8 : 1, and tested with a cross-head speed of 1 mm min^{-1}. These samples were used to obtain a general view of the effect of several of the variables. The shear strength was plotted against different combinations of the shear length L and the thickness of the sheets. Although several of these combinations gave trends for the thick sheets (> 1 mm) and/or for the thin sheets (< 0.5 mm), the relationships usually broke down when the whole range of thickness was taken together. On the other hand, Figs 6a and b show that the shear strength of the sheets decreases with increasing shear length L, and this trend applies for sheet thicknesses between 0.06 mm up to 3.20 mm. Within the observed scatter the shear strength is independent of the method of drawing and of the parent material. Irradiation after drawing has no effect on the results.

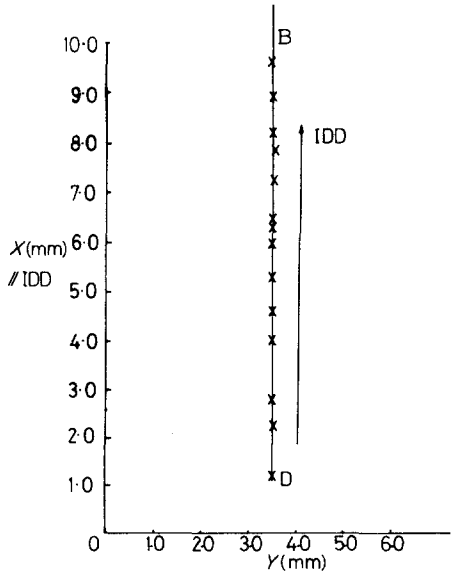

Figure 5 Determination of the direction of the deformation band. Coordinates X and Y of the maxima of the shear strain across the band. X is parallel to the IDD.

Samples were also irradiated before drawing with doses of 0.6 and 6.0 Mrad. These sheets were all die drawn up to a maximum draw ratio of 9.5 : 1 for the lower irradiation dose and 7.7 : 1 for the higher irradiation dose. These samples are not, therefore, included in the results seen in Fig. 6. However, comparison of these samples with unirradiated samples drawn to similar draw ratios shows that irradiation before drawing up to a dose of 6.0 Mrad does not affect the shear strength of the drawn sheets.

Next, we studied the effect of draw ratio and cross-head speed on the shear strength of the sheets. Because of the results presented above, these comparisons are made at constant nominal shear length L.

Figs 7a, b and c show that the shear strength increases with drawn ratio. Figs 8a, b and c show that the shear strength increases with increasing cross-head speed.

The points in Figs 6b, 7 and 8 are averages and the errors quoted are σ_{n-1}. The numbers at the top of the error range give the number of samples involved. When only one sample is available, the symbols for Fig. 6a apply.

The increase of the shear strength with increasing deformation rate reflects the well-known fact that yield is a thermally activated rate process. On the other hand, the effect of draw ratio is somewhat

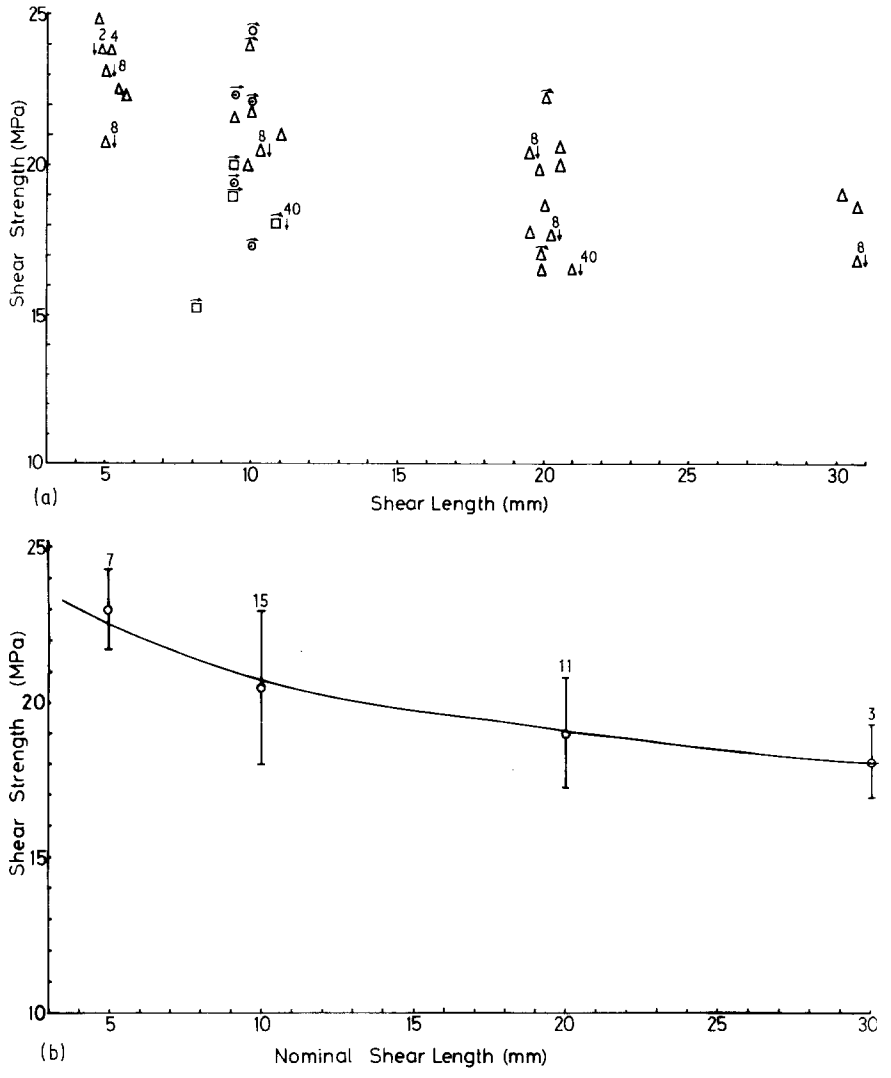

Figure 6 Shear strength plotted against shear band length (L) for samples with draw ratios between 10.0 : 1 and 11.8 : 1. Deformation rate: 1 mm min^{-1}. (a) Individual measurements: (△) die drawn sheets, Hizex 7000F, (⊙) Instron drawn sheets, Hizex 7000F, (□) Instron drawn sheets, BP006/60, (⇝) thin sheets with plates, (→) thin sheets without plates, (↓) irradiated after drawing (the numbers indicate the dose in Mrad). (b) Averages for nominal values of L. Numbers above each point indicate the number of samples included in each average. Errors are $\pm\sigma_{n-1}$.

surprising because higher orientation might, a priori, be expected to be associated with easier shear along the molecular orientation direction. However, Ladizesky *et al.* [13] elaborated on ideas of Peterlin, Geil, Keller and others [14] and considered that, on drawing, the spherulites of the isotropic polymer transform into a fibrillar structure. The fibrils involve crystalline blocks alternating with non-crystalline material, and contain taut-tie molecules [14] and/or crystalline bridges [15]. Furthermore, individual "wandering" molecules are sheared by two or more fibrils of the final draw material, and maintain a degree of overall lateral cohesion.

As suggested in [13], the "wandering" molecules and the van der Waals forces are mostly responsible for the shear strength along the orientation direction. The increase of shear strength with increasing draw ratio may, therefore, be due to the resultant tightening-up of these molecules.

The insensitivity of the shear strength to irradiation supports the conclusions obtained from pull-out tests, and presented earlier [13]. The explanation advanced there may now be expanded as follows: for irradiation before drawing, the cross-links are largely confined to the spherulites of the isotropic polymer. On drawing, the cross-links remain within individual fibrils (macro-

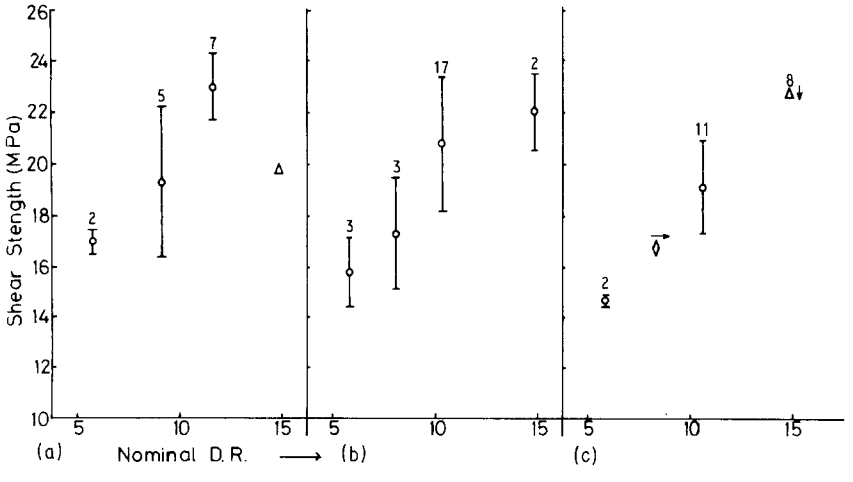

Figure 7 Shear strength plotted against nominal draw ratio for different nominal band length L. When no range of errors ($\pm\sigma_{n-1}$) is given, the points correspond to individual measurements. All details and symbols as in Fig. 6 plus: (◇) die drawn sheets, BP006/60. (a) Nominal L = 5 mm, (b) nominal L = 10 mm, (c) nominal L = 20 mm.

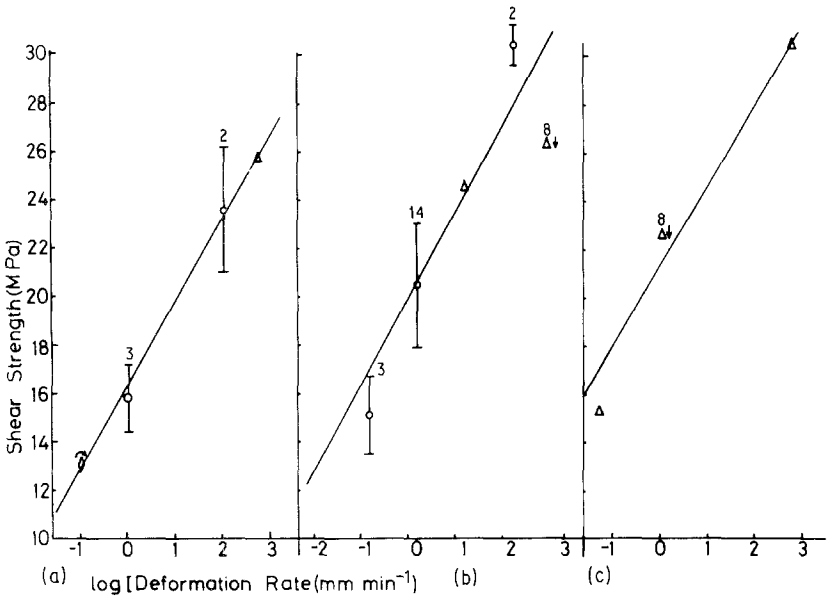

Figure 8 Shear strength plotted against deformation rate for different draw ratios and nominal deformation band length L. All details and symbols as for Figs 6 and 7. (a) Draw ratios between 5.6:1 and 5.9:1. Nominal L = 10 mm. (b) Draw ratios between 10.0:1 and 11.8:1. Nominal L = 20 mm. (c) Draw ratio 14.7. Nominal L = 20 mm.

fibrils) and the "wandering" molecules are little or not affected. For irradiation after drawing, cross-linking takes place in the oriented, non-crystalline regions within the macro-fibrils, and the "wandering" molecules are, again, largely unaffected. It follows that irradiation before or after drawing should not affect the shear strength results, as found in our experiments.

It is of interest at this stage to refer to Fig. 9, showing the shear strain, γ, along the deformation band. Each curve corresponds to a different sample and the relevant data may be seen in Table I. The sample corresponding to Fig. 9e has been irradiated after drawing but, in all other respects, it is identical to the sample corresponding to Fig. 9a. In particular, both samples have been deformed up to point A of Fig. 2. It may be seen that the irradiated sample shows the smallest shear strain, γ, that is, it has the largest recovery from the final deformation. This suggests that our experiments involve contributions from cross-linking, a conclusion that appears to contradict the ideas advanced above. However, the situation may be rationalized as follows.

Fig. 2 shows that the shear strength of all our samples relates to the yield stress. This process has been associated above with shear between fibrils, controlled by the "wandering" molecules and by van der Waal's forces. This gives shear strength values which are largely unaffected by irradiation.

The amorphous regions, where the cross-linking takes place, are not involved in the yield process. However, these regions may still contribute to deformations which can take place within the fibrils (e.g. intralamellar shear). In this case, a cross-linked network should produce a larger recovery than an uncross-linked network, as shown by our results. A future publication will present further examples and discussion on the effect of irradiation on the shear strain of HDLPE sheets along their orientation direction.

3.2. Shear strength measurements: consideration in terms of the behaviour of lap joints

It was pointed out to us by Dr G. R. Davies that the measurement of shear strength for these samples, where the deformation is concentrated into a narrow parallel strip of material undergoing simple shear, is closely analogous to the adhesive failure of a lap joint [16–18]. A typical lap joint is shown schematically in Fig. 10, where the strip of adhesive of thickness, h_0, corresponds to the shear band. Fig. 11 shows the cross-section, first in the undeformed state (a), and with increasing deformation under the applied tensile force, (b) and (c).

At the centre of the adhesive both adherents are bent away from the adhesive, and the adherents will develop elastic stresses which will compress the adhesive. At the ends M and N of the adhesive strip (Fig. 11c), on the other hand, the adhesive is under tensile stress, and there will be a strong tendency to peel. This occurs because of the flexibility of the adherents, and it is here that the system is most likely to fail, rather than in the compressive region at the centre of the lap joint.

TABLE I Data related to Fig. 9

Fig. 9 Thickness	Material	Method of Drawing & Nominal Draw Ratio	Nominal L (mm)	Deformation up to (Point in Fig. 2)	Def. Rate (mm min^{-1})
(a) Thin	Hizex 7000F	Instron 10.0:1	10	A	1
(b) Thin	BP006/60	Die Draw 5.6:1	10	B	1
(c) Thin	Hizex 7000F	Die Draw 5.6:1	20	A	0.1
(d) Thick	Hizex 7000F	Die Draw 10.0:1	30	B	1
(e) Thin	Hizex 7000F*	Instron 10.0:1	10	A	1

*Irradiated after drawing. Dose: 40 Mrad, low dose rate.

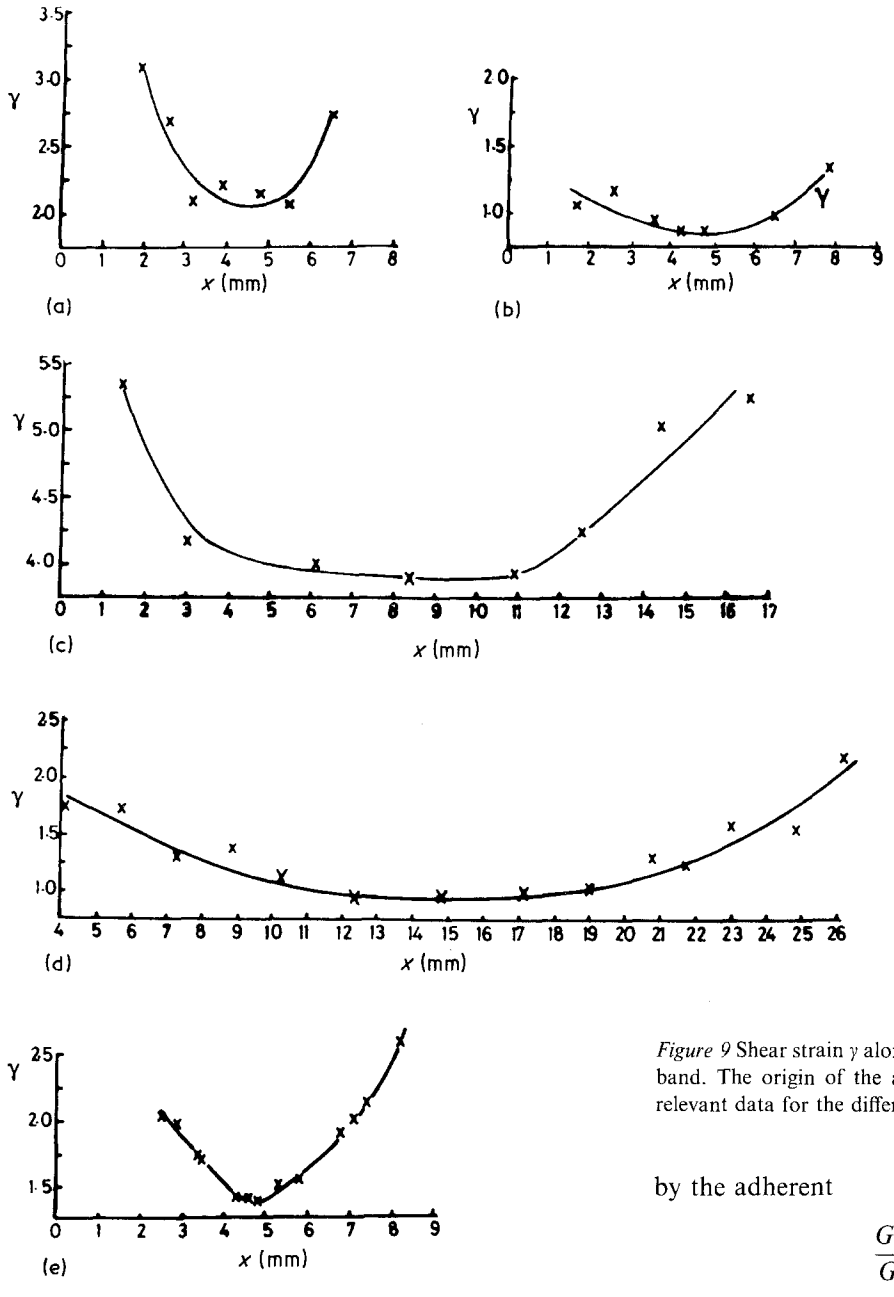

Figure 9 Shear strain γ along the "centre" line x of the deformation band. The origin of the absissa is taken at the band edge. The relevant data for the different samples is given in Table I.

The distribution of tensile stresses and shear stress referred to the schematic diagram of Fig. 12 are shown in Fig. 13 for very small external stresses, according to the idealised calculations of Goland and Reissner [16]. This figure shows σ_0, the stress in the adhesive perpendicular to the plane of the lap joint, σ_f the tensile stress in the adherent adjoining the adhesive (in the direction of the external stress $f_0 = F_0/\delta w$) and τ_0, the shear stress in the adhesive, as a function of the distance from the joint edge. This distance is defined non-dimensionally as the distance from the joint edge divided by δ.

The stress distribution shown in Fig. 13 is strictly only valid provided that the adherents are thin plates and the following inequalities are satisfied.

$$h_0 \ll \delta < l + L/2 \tag{1}$$

$$\left[\frac{f_0\delta}{D_1}\right]^{1/2} l \gg 1 \tag{2}$$

and where the flexibility of the lap joint is controlled by the adherent

$$\frac{G_1}{G} \gg \frac{h_0}{\delta} \ll \frac{E_1}{E} \tag{3}$$

In these equalities, D_1 is the flexural rigidity of the adherent, G_1 and E_1 are the shear modulus and tensile modulus of the adhesive, G and E the corresponding properties of the adherent.

In the present experiment, the Inequality 1 is readily satisfied. This is also true for Inequality 3 on the basis that $G_1 = G$ and $E_1 = E$. Calculations show that $[f_0\delta/D_1]^{1/2} l$ is of the order of 0.2, so that the actual stress distributions are likely to differ in detail from those shown in Fig. 13. Nevertheless, we shall find that the principal qualitative conclusions are relevant to our results for shear of the polyethylene sheets. According to Fig. 13, the Goland and Reissner theory predicts that the peeling stress σ_0/f_0 is large and positive at the edge of the joint but becomes negative as we approach the centre of the overlap region. Furthermore, the maximum values of peeling stress and tensile stress occur at the edges of the overlap, whereas the maximum value of the shear stress in the central strip (the shear band) occurs close to, but not quite consistent with, the edge of the overlap.

In our experiments we are interested in the relationship between the greatest values of the stresses σ_f, σ_0

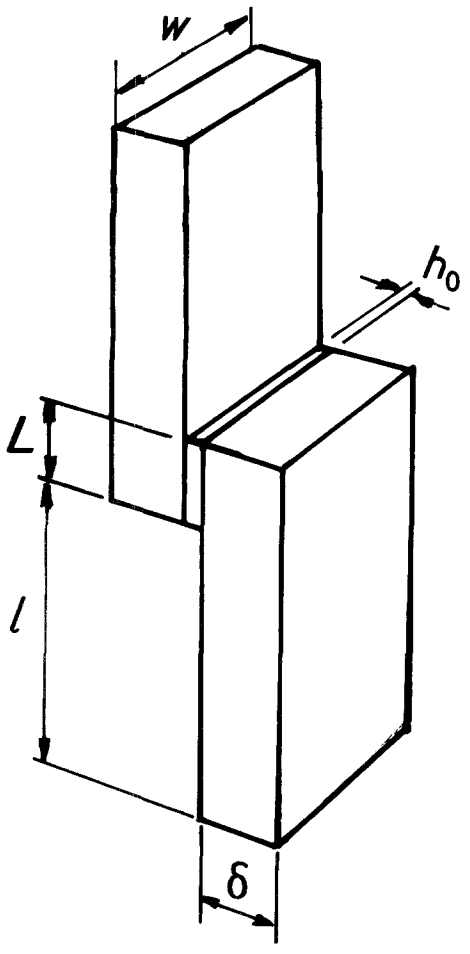

Figure 10 Lap joint sample showing the nomenclature used in the text.

and τ_0 and the value of f_0, which is increased until the lap joint breaks down. According to the theory of Goland and Reissner [16] these relationships depend on a nondimensional parameter k which decreases from 1.00 to 0.26 as the nondimensional ratio $(L/\delta)(f_0/\delta E)^{1/2}$ increases. Fig. 14 shows the maximum stress values with decreasing values of k, that is, with increasing f_0. It may be seen that the peeling stress σ_0 can be 4.3 times the applied external stress f_0. Although σ_0/f_0 decreases with increasing f_0, it can be shown that the peeling stress $[\sigma_0]_{max}$ actually increases with f_0. We are also interested in the dependence of the shear strength of the sample on the overlap length L. Maintaining E, δ and f_0 constant, the parameter k decreases with increasing L and Fig. 14 shows that

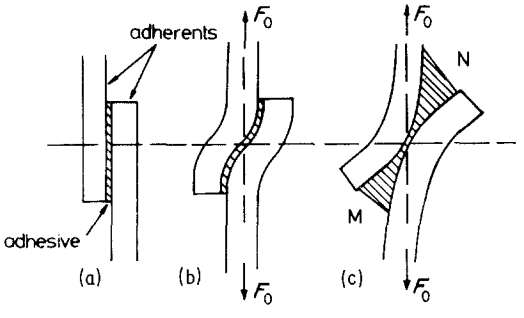

Figure 11 Deformation of a flexible lap joint, (a) before application of external force, (b) after application of an external tensile force, F_0, (c) close to failure. From [18].

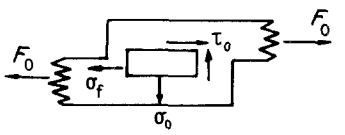

Figure 12 System of stresses on the overlap of a lap joint after the application of an external tensile force, F_0.

σ_0/f_0, etc., are smaller. Thus, the shear strength decreases as L increases.

In summary, the theoretical predictions suggest (a) failure should initiate at the edges of the overlap region, through a peeling off mechanism, (b) the shear strength should decrease with increasing L, (c) the shear stress is maximum near the ends of the overlap region and decreases towards the centre of the sample.

Three experimental observations were always present in our work.

(a) All our samples show splitting at each end of the deformation band. Fig. 15 shows examples covering a wide range of variables, and these are shown in Table II. In particular, note that the splitting is also observed in Fig. 15a corresponding to a sample whose deformation was stopped well before the maximum load has been achieved (point C in Fig. 2). In this case the shear band is virtually non-existent, that is, the deformation up to this point has been recoverable to a large extent. These results are in full agreement with the theoretical prediction (a) above.

SEM observations provide further evidence of the mechanisms contributing to the deformation of the band, namely "peeling" failure at the edges and simple shear inside the band.

The deformation of some thick and thin sheets was continued until complete separation occurred, and the free surfaces in the shear region were then examined under the SEM. In these cases the shear strain may be considered infinite, and the large plasticity of the samples will produce large localized deformation, which might not be fully compatible with the mechanisms operating around point B in Fig. 2. Nevertheless, Fig. 16 shows the free surfaces of the shear region of thick and of thin sheets. The relevant data for these samples may be seen in Table III. For the thick sheets, Fig. 16a shows a significant amount of tear, occurring

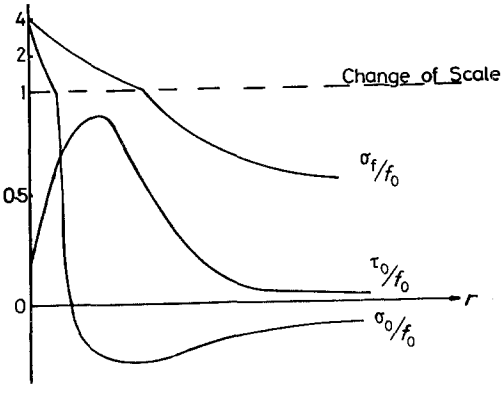

Figure 13 Lap joint theory for small applied stress f_0. Distribution of tensile and shear stresses along the deformation band, normalized with f_0. r is the distance from the overlap edge divided by δ. From [17].

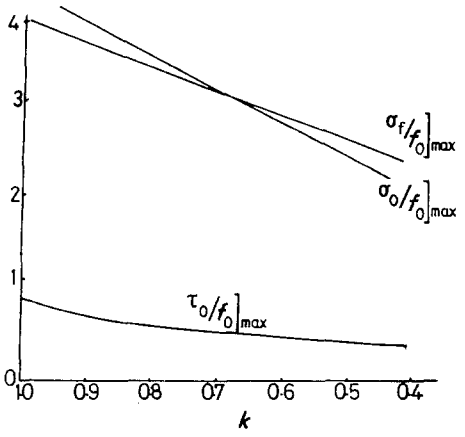

Figure 14 Lap joint theory. Maximum stresses normalized with f_0, as a function of the non-dimensional factor k (see text). From [16].

preferentially near the edges of the shear band. Away from these edges the surfaces are clearly produced by shear failure, as seen in Fig. 16b. For the thin sheets a similar situation applies (Figs 16c and d), but in this case the tear failure extends deeper into the middle of the shear band. This is because in-plane bending of the thin sheets, clamped at the top with a universal link, was significantly larger than for the thick sheets, which were clamped with rigid links at both ends.

(b) The lap joint theory predicts a decrease of the shear strength with increasing overlap L. This prediction is fulfilled in our experiments, as seen in Figs 6a and b.

(c) The lap joint theory predicts maximum values of shear stress close to the edge of the overlap, and decreasing towards the centre. In our experiments we did not measure the shear stress but, instead, we measured the shear strain along the middle line of the band length. The results are seen in Fig. 9 for both thin and thick samples. It is seen that the shear strain in our experiments follows the trend which the lap joint theory predicts for the shear stress. Qualitatively, both trends are equivalent because our results apply to all levels of deformation, including samples where the deformation was stopped just after the maximum load has been achieved (point C in Fig. 2).

4. Conclusions

The shear strength of HDLPE sheets in the draw direction is significantly affected by the draw ratio and by the deformation rate, but irradiation produces no measurable effect. All the main characteristics of the shear deformation of our lap joint type samples are qualitatively predicted by lap joint theory.

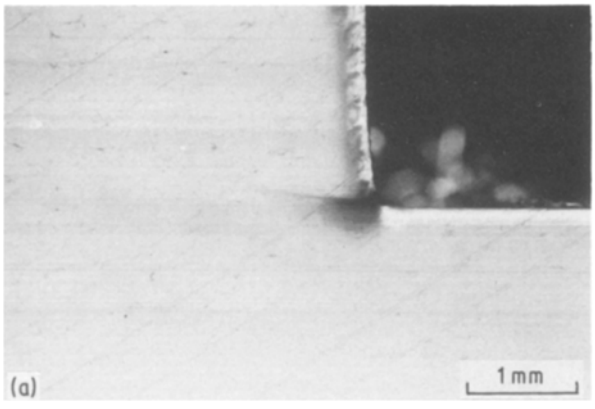

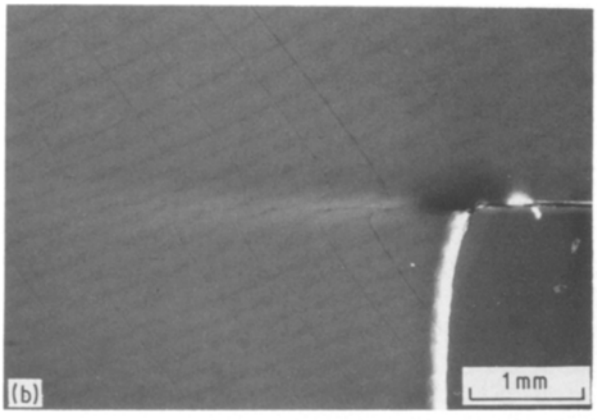

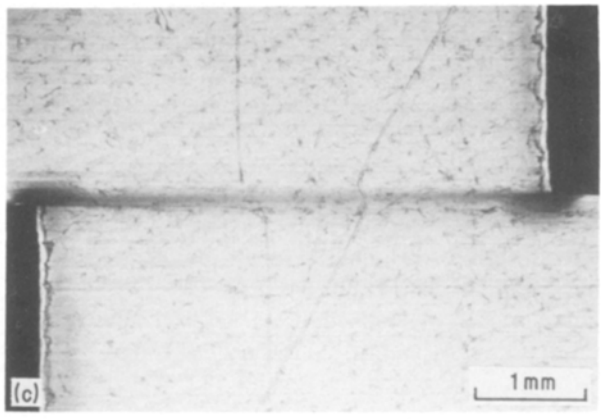

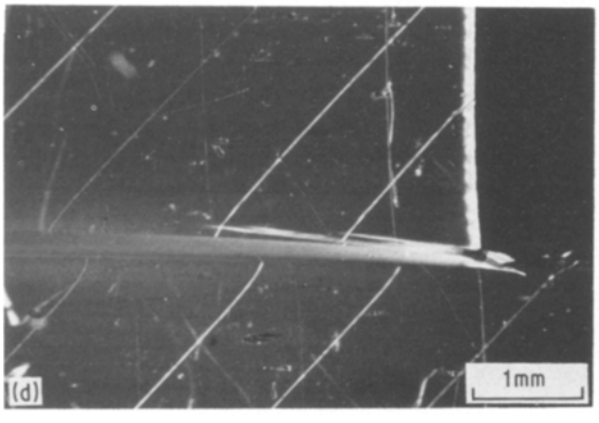

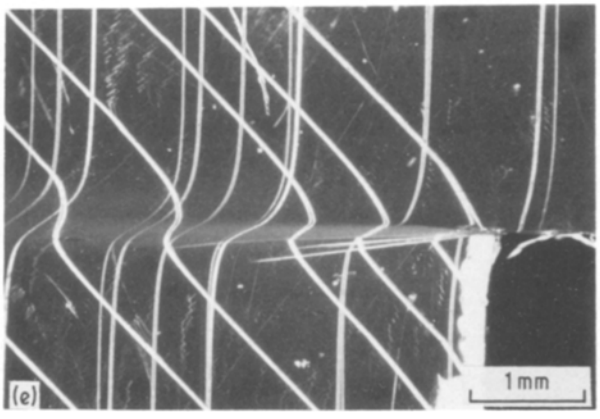

Figure 15 Photographs of edges of deformation bands for different samples. The relevant data may be seen in Table II.

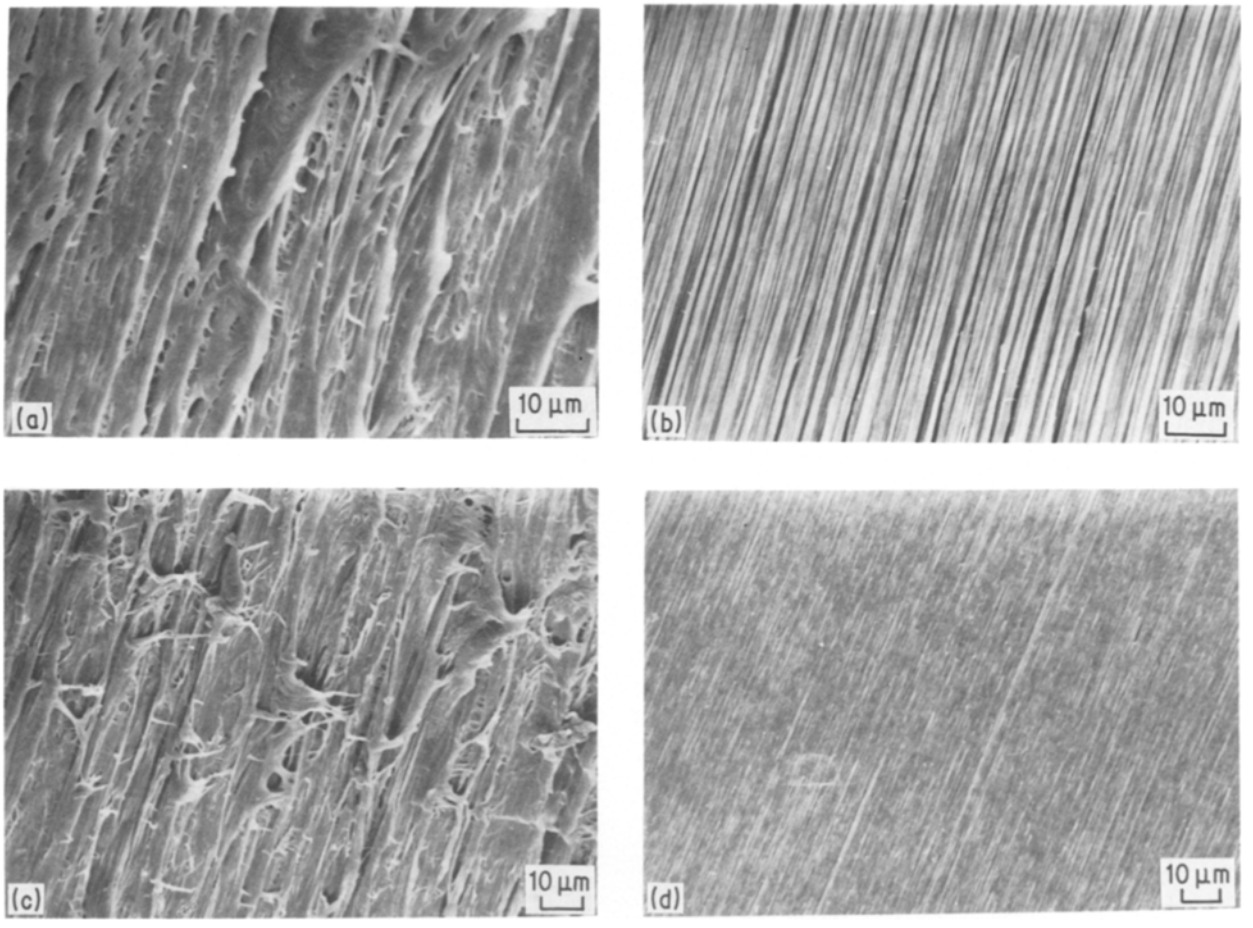

Figure 16 Scanning electron micrographs of deformation band surfaces for samples sheared until complete separation occurred. The relevant data may be seen in Table III.

Acknowledgements

We are grateful to Mr Yuan Chaoting for the careful and painstaking measurement of the shear strains and associated computing work. The electron irradiation of our samples was carried out at the Cookridge Radiation Research Centre, University of Leeds, by courtesy of Drs G. A. Salmon and F. Wilkinson. γ-irradiation was performed with facilities provided by the School of Chemistry, University of Leeds, by courtesy of Dr E. Collinson. Dr M. G. Dobb, Department of Textile Industries, The University of Leeds, provided the scanning electron microscope, and Mr T. Buckley gave technical assistance with this instrument. Dr A. Selwood supplied the die-drawn polyethylene sheets, and Mr D. Armitage patiently prepared the many dozens of samples required in this work.

TABLE II Data related to Fig. 15

Fig. 15 Thickness	Material	Method of Drawing & Nominal Draw Ratio	Nominal L (mm)	Deformation up to (Point in Fig. 2)	Def. Rate (mm min^{-1})
(a) Thick	Hizex 7000F	Die Draw 11.0 : 1	20	C	1
(b) Thick	Hizex 7000F*	Die Draw 7.7 : 1	10	B	1
(c) Thick	Hizex 7000F	Die Draw 6.0 : 1	5	B	0.05
(d) Thin	BP006/60	Die Draw 5.6 : 1	10	A	100
(e) Thin	Hizex 7000F†	Instron 10.0 : 1	10	A	1

*Irradiated before drawing. Dose: 6 Mrad, high dose rate.
†Irradiated after drawing. Dose: 40 Mrad, low dose rate.

TABLE III Data related to Fig. 16

Fig. 16 Thickness	Material	Method of Drawing & Nominal Draw Ratio	Nominal L (mm)	Deformation up to (Point in Fig. 2)	Def. Rate (mm min^{-1})
(a) Thick	Hizex 7000F	Die Draw	10	1	Edge
(b) Thick		11.0 : 1			Centre
(c) Thin	Hizex 7000F	Instron	10	1	Edge
(d) Thick		8.0 : 1	10	1	Centre

References

1. I. M. WARD, *Adv. Polym. Sci.* **70** (1985) 1.
2. G. CAPACCIO and I. M. WARD, *Polym. Eng. Sci.* **15** (1975) 219.
3. P. SMITH and P. J. LEMSTRA, *J. Mater. Sci.* **15** (1980) 505.
4. A. G. GIBSON, I. M. WARD, B. N. COLE and B. PARSONS, *ibid.* **9** (1974) 1193.
5. B. PARSONS and I. M. WARD, *Plastics Rubber Proc. Appl.* **2** (1982) 215.
6. N. H. LADIZESKY and I. M. WARD, *J. Mater. Sci.* **18** (1983) 533.
7. L. E. ALEXANDER, "X-Ray Diffraction Methods in Polymer Science" (Wiley, New York, 1969) Ch. 5.
8. N. BROWN and I. M. WARD, *Philos. Mag.* **17** (1968) 961.
9. I. D. RICHARDSON, R. A. DUCKETT and I. M. WARD, *J. Phys. D Appl. Phys.* **3** (1970) 649.
10. N. BROWN, R. A. DUCKETT and I. M. WARD, *Br. J. Appl. Phys. (J. Phys. D)* **1** Ser 2 (1968) 1369.
11. *Idem, Philos. Mag.* **18** (1968) 483.
12. R. A. DUCKETT, B. C. GOSWAMI and I. M. WARD, *J. Polym. Sci. Polym. Phys. Edn* **15** (1977) 333.
13. N. H. LADIZESKY, Y. CHAOTING and I. M. WARD, *J. Macromol. Sci. Phys.* **B25** (1, 2) (1986) 185.
14. A. PETERLIN, *J. Mater. Sci.* **6** (1971) 490.
15. A. G. GIBSON, G. R. DAVIES and I. M. WARD, *Polymer* **19** (1978) 683.
16. M. GOLAND and E. RIESSNER, *J. Appl. Mech.* **11** (1944) 17.
17. D. D. ELEY (ed.) "Adhesion" (Oxford University Press, London, 1961) Ch. IX.
18. J. J. BIKERMAN, "The Science of Adhesive Joints", 2nd Edn (Academic, New York, 1968) Ch. VIII.

Received 8 December 1986
and accepted 28 January 1987